

Incorporating temperature-sensitive Q_{10} and foliar respiration acclimation algorithms modifies modeled ecosystem responses to global change

Kirk R. Wythers,¹ Peter B. Reich,^{1,2} and John B. Bradford³

Received 28 October 2011; revised 24 October 2012; accepted 27 October 2012.

[1] Evidence suggests that respiration acclimation (RA) to temperature in plants can have a substantial influence on ecosystem carbon balance. To assess the influence of RA on ecosystem response variables in the presence of global change drivers, we incorporated a temperature-sensitive Q_{10} of respiration and foliar basal RA into the ecosystem model PnET-CN. We examined the new algorithms' effects on modeled net primary production (NPP), total canopy foliage mass, foliar nitrogen concentration, net ecosystem exchange (NEE), and ecosystem respiration/gross primary production ratios. This latter ratio more closely matched eddy covariance long-term data when RA was incorporated in the model than when not. Averaged across four boreal ecotone sites and three forest types at year 2100, the enhancement of NPP in response to the combination of rising $[\text{CO}_2]$ and warming was 9% greater when RA algorithms were used, relative to responses using fixed respiration parameters. The enhancement of NPP response to global change was associated with concomitant changes in foliar nitrogen and foliage mass. In addition, impacts of RA algorithms on modeled responses of NEE closely paralleled impacts on NPP. These results underscore the importance of incorporating temperature-sensitive Q_{10} and basal RA algorithms into ecosystem models. Given the current evidence that atmospheric $[\text{CO}_2]$ and surface temperature will continue to rise, and that ecosystem responses to those changes appear to be modified by RA, which is a common phenotypic adjustment, the potential for misleading results increases if models fail to incorporate RA into their carbon balance calculations.

Citation: Wythers, K. R., P. B. Reich, and J. B. Bradford (2013), Incorporating temperature-sensitive Q_{10} and foliar respiration acclimation algorithms modifies modeled ecosystem responses to global change, *J. Geophys. Res.: Biogeosci.*, 118, doi:10.1029/2011JG001897.

1. Introduction

[2] Autotrophic respiration accounts for $\approx 60 \text{ Gt C yr}^{-1}$, or roughly half of the total carbon (C) released annually by the terrestrial biosphere [Schlesinger, 2005]. This is a large number relative to global CO_2 emissions from fossil fuel burning, which are ≈ 7 to 8 Gt C yr^{-1} . The combination of land and ocean C sinks, together with fossil fuel emissions and deforestation, have conservatively increased atmospheric $[\text{CO}_2]$ by 30% over the last 200 years [Keeling and Whorf, 1995; Le Quere et al., 2010], with such increases

expected to continue, or grow, in the future [Le Quere et al., 2010]. As a result, increases of 4°C to 7°C in global surface temperature means are anticipated by year 2100 [Christensen et al., 2007; Intergovernmental Panel on Climate Change, 2008]. Realistic estimates of plant respiration's response to global change drivers will be necessary to develop accurate predictions of regional C balances, and these will be important given the potentially large feedbacks on atmospheric $[\text{CO}_2]$ from terrestrial ecosystems. In this article, we incorporate a temperature-sensitive Q_{10} of respiration and a foliar basal respiration acclimation algorithm (collectively referred to as respiration acclimation (RA) herein) into an ecosystem model to assess impact of RA on net primary production (NPP), total canopy foliage mass, and foliar nitrogen (N) concentration, in the presence of global change drivers.

[3] Process-based models, which are constructed at the tissue level of organization (i.e., leaf, stem, and root), are often used to examine the relationships between environmental change and ecosystem function. Models that simulate system behavior in terms of C balance typically do so with a collection of interactive algorithms that estimate C assimilation, respiration, and allocation. This article focuses on the

All Supporting Information may be found in the online version of this article.

¹Department of Forest Resources, University of Minnesota, Saint Paul, Minnesota, USA.

²Hawkesbury Institute for the Environment, University of Western Sydney, Penrith, New South Wales, Australia.

³U.S. Geological Survey, Southwest Biological Science Center, Flagstaff, Arizona, USA.

Corresponding author: K. R. Wythers, University of Minnesota, Department of Forest Resources, 115 Green Hall, 1530 Cleveland Ave. N., Saint Paul, MN 55108, USA. (kwythers@umn.edu)

©2012. American Geophysical Union. All Rights Reserved.
2169-8953/13/2011JG001897

respiration side of that equation, where the challenge in representing plant respiration in a mathematical model is in appropriately incorporating the multiple sources of variation that impact plant respiration.

[4] Temperature is an important regulator of many biological processes, including respiration. The influence of temperature is often expressed exponentially, following van't Hoff's reaction rate-temperature rule. One such relationship is the respiration-temperature response function. An example of the respiration-temperature response function that allows for the direct estimation of the Q_{10} parameter and can also be used to estimate the respiration rate at one temperature from the respiration rate at a lower temperature is:

$$R_d = R_{d_{ref}} Q_{10}^{\frac{T - T_{ref}}{10}}, \quad (1)$$

where temperatures are in Celsius degrees, and Q_{10} is the ratio between respiration rate at one temperature and the respiration rate 10°C lower [Atkin and Tjoelker, 2003; Larcher, 2003; Tjoelker et al., 1999a]. Many carbon balance models calculate their respiration estimates with fixed Q_{10} and constant $R_{d_{ref}}$ as a proportion of photosynthesis [Aber et al., 1995, 1996; Cramer et al., 1999; Kicklighter et al., 1999; Lou et al., 2008; Potter et al., 2001; Sampson et al., 2006; Sitch et al., 2008; Zaragoza-Castells et al., 2008]. Although this approach has some basis in empirical observations [e.g., Reich et al., 1998b; Wright et al., 2004], it suffers from being inexact and distant from the fundamental underlying biology.

[5] Plant respiration responses to temperature change often do not follow a simple exponential Q_{10} [Atkin et al., 2006, 2008; Larcher, 2003; Tjoelker et al., 2009]. In particular, the response of dark respiration to short-term temperature fluctuations may depart substantially from a simple exponential function [Tjoelker et al., 2001, 2009]. In addition, changes in long-term temperature conditions may alter the basal respiration term of the temperature response function [Atkin and Tjoelker, 2003; Tjoelker et al., 2008]. These are potentially important, yet typically absent components of C balance calculations in many mathematical models. The assumption in many ecosystem models that respiration increases exponentially with temperature and does not thermally acclimate is not due to a consensus that an exponential response with no acclimation best represents respiration's response to changing temperature, but rather a lack of agreement as to how to better represent respiration's response to a changing thermal environment.

[6] Although respiration responds to temperature on both short- and long-term time scales, the Q_{10} of respiration (as used herein) describes the short-term sensitivity of respiration to temperature. The near-instantaneous exponential respiration function described by a single Q_{10} value has been shown to inadequately fit empirical observations in plants [Belehrádek, 1930; Wager, 1941] (see reviews by Berry and Raison [1981], Forward, [1960], and James [1953]) and in soils [Lloyd, 1999]. Tjoelker et al. [2001] showed that the near-instantaneous respiration-temperature response across a broad range of plant taxa could be better fit with a function whose exponent varied with temperature, with dark respiration showing decreasing Q_{10} values with increasing measurement temperature.

[7] In addition to short-term temperature response, respiration rates are known to thermally acclimate over longer time periods by shifting the overall elevation and/or shape of the temperature-response function. Respiratory C exchange rates are known to acclimate with time to prevailing temperatures in plant leaves [Atkin et al., 2000, 2008; Tjoelker et al., 1999a, 1999b, 2008, 2009], roots [Atkin et al., 2009; Gunn and Farrar, 1999; Tjoelker et al., 1999a], and perhaps soil microbes or mycorrhizal fungi [Bradford et al., 2008; Malcolm et al., 2008]. The acclimation response can be large [Gunderson et al., 2000] and rapid [Atkin et al., 2000; Bolstad et al., 2003], and therefore have a substantial influence on ecosystem C balance. Acclimation to temperature may result from an alteration in the temperature-sensitive Q_{10} , a shift in the elevation of the temperature-response function (i.e., its intercept, often represented by the so-called basal respiration rate), or both [Atkin and Tjoelker, 2003; Atkin et al., 2000; Tjoelker et al., 1999a], although most evidence supports a shift in the basal rate. This shift typically results in lower realized respiration at a standard temperature in warm acclimated plants relative to cold acclimated plants. Consequently, the respiration response to long-term changes in the thermal environment will likely differ from predictions based on short-term temperature-response functions.

[8] Although many modelers recognize the imperfections of the Q_{10} relationship, fixed nonacclimating respiration parameters are still in wide use, because until recently, there has not been a clear and generalizable alternative. Wythers et al. [2005] reviewed a number of ecosystem models and reported that 16 of 19 models examined used a static Q_{10} parameter, a static R_d parameter, or both. Moreover, despite evidence of thermal acclimation of $R_{d_{ref}}$, none of those models included acclimation. Other models do not calculate respiration at all, but assume NPP at stand to landscape scales is a fixed proportion of gross primary production [Coops and Waring, 2001; Waring and McDowell, 2002; Waring et al., 1998]. However, the approach may fail to account for site-level climatic and plant functional variation, and evidence suggests that this value would not likely be a fixed proportion [DeLucia et al., 2007]; in addition, there is no empirical evidence or theoretical basis to extend this approach to novel thermal regimes.

[9] Recently, several ecosystem models were modified to incorporate thermal acclimation of respiration into their C accounting algorithms [Atkin et al., 2008; King et al., 2006; Wythers et al., 2005], with pronounced impacts on modeled C flux. This article builds on and expands the prior work in several key ways. It is important to highlight differences in approach to model alteration, in the nature and scale of models used, in the target study system, and in model scenarios, because the diversity of approaches suggests that we are far from a comprehensive coverage of this topic. Each of the prior publications modified respiration in relation to temperature in different ways and using relationships based on different empirical data sets. First, Wythers et al. [2005] used data from field observations of both gymnosperm and angiosperm trees, King et al. [2006] used "empirical observations from plant warming experiments," and Atkin et al. [2008] used data for seedlings of 19 species grown in controlled environmental conditions in the laboratory. Second, the three studies examined impacts of RA

on carbon balance under either current static conditions [Wythers *et al.*, 2005], a single future climate-CO₂ change scenario [King *et al.*, 2006], or under all pairwise combinations of static and dynamic global vegetation with 1861 or modeled 2100 coupled climate-CO₂ scenarios [Atkin *et al.*, 2008]. Third, Atkin *et al.* [2008] tested impacts of RA but did not incorporate a temperature-sensitive Q_{10} into the model, whereas the other studies did. Fourth, Wythers *et al.* [2005] examined responses of four species terrestrial ecosystem types, whereas the other two articles reported results of global models.

[10] This article builds on this diverse but rudimentary foundation by examining regional scale differences for specific forest types and climate regimes, with a focus on separating impacts of incorporation of RA under climate warming versus elevated CO₂, and incorporating historic climate variability into the scenario. As the only one of the three prior publications that explicitly compared impacts of improved respiration modeling on C balances under contrasting global environmental change scenarios, Atkin *et al.* [2008] used different equations for RA than in our model, examined responses for coupled changes in CO₂ and climate, and reported results at the global scale. We believe that our results provide a second, complementary assessment of impacts of RA on modeled C cycle consequences, which should be followed by others until a well-validated consensus has been reached in the community. Finally, none of the aforementioned models, however, examined RA effects in conjunction with rising CO₂ and temperature, both individually and in combination, the interactions of which may produce nonintuitive consequences. Our research specifically addresses this issue.

[11] In addition, as far as we are aware, ours is the first modeling study to examine RA impacts using global change drivers that include their historic variability. We know from experiments with rainfall variability that variability alone can alter ecosystem responses [Fay, 2009; Heisler-White *et al.*, 2008, 2009; von Wehrden *et al.*, 2010]. Therefore, given the importance of temperature sensitivity of respiration, assessing the effects of RA under a range of realistic future climate scenarios should be of value.

[12] To accomplish the above goals, we incorporated RA algorithms into PnET-CN, a version of the PnET model that includes not only belowground temperature-response functions, but also adds live biomass, litter, and belowground organic pools, along with adding N to all compartments and fluxes. These changes allow for dynamic foliar N estimates, and CO₂-stomatal conductance response functions [Ollinger *et al.*, 2002]. We ran the simulation within a Monte Carlo climate generator based on historical climate variability. We evaluated the effects of RA algorithms on NPP, foliage mass, foliar N, and net ecosystem exchange (NEE) in the presence of CO₂ and temperature interactions within simulated climate change scenarios, for three forest types, at a range of sites. We chose sites representing the north-south and east-west margins of the temperate-boreal forest ecotone at the center of the North American continent, a forested region expected to undergo substantial change [Frelich and Reich, 2010] under most future climate predictions (Figure 1). All three forest types (aspen, pine, and spruce) occur in all four regions; hence, our study allows us to address responses of forest type, climate zone, and possible interactions. We focus largely on NPP and its drivers, canopy foliage mass and foliar N, because modeling



Figure 1. Study site locations: Detroit Lakes, Minnesota (46.8°N,95.8°W)—southwest (DL); Sioux Lookout, Ontario, Canada (50.1°N,91.5°W)—northwest (SL); Kapuskasing, Ontario, Canada (49.4°N,82.4°W)—northeast (KA); and Mount Pleasant, Michigan (43.6°N,84.8°W)—southeast (MP).

of NEE is much more uncertain and involves accurate temperature response algorithms for soil respiration, which is likely beyond the capabilities of any ecosystem model [Mahecha *et al.*, 2010; Reich, 2010].

2. Methods

2.1. Sites

[13] We compared NPP, foliar mass, foliar N, and NEE from model simulations run with both static respiration parameters and alternative, variable RA algorithms across a range of vegetation types and sites under: (1) current ambient conditions, (2) rising [CO₂], (3) warming, and (4) rising [CO₂] with warming. We modified PnET-CN site parameters [Aber *et al.*, 1997] to represent a range of temperate-boreal forest sites in the upper midwest of the North American continent: (1) Detroit Lakes, Minnesota, USA (46.81°N 95.86°W), representing the Southwestern corner (DL); (2) Sioux Lookout, Ontario, Canada (50.09°N 91.91°W), representing the Northwestern corner (SL); (3) Kapuskasing, Ontario, Canada (49.42°N 82.45°W), representing Northeast corner (KA); and (4) Mount Pleasant, Michigan, USA (43.62°N 84.76°W), representing the Southeast corner (MP) (Figure 1). We developed vegetation parameters for aspen (aspen), black spruce (spruce), and jack pine (pine) following Aber *et al.* [1997] with data from Reich *et al.* [1998a, 1998c, 1999] and Tjoelker *et al.* [2008]. See Tables 2 and 3 for site and vegetation parameter values.

2.2. Climate

[14] We used measured climate from the Midwest Regional Climate Center (Champaign, Ill.) and the Canadian National Climate Data and Information Archive (Fredericton, New Brunswick). We calculated means for mean annual temperature, mean photosynthetically active radiation (PAR), and

mean annual precipitation (Table 1), and monthly means and covariances for maximum and minimum temperature, PAR, and precipitation over the available climate record (Detroit Lakes: n = 107 years; Sioux Lookout: n = 71 years; Kapuskasing: n = 72 years; and Mount Pleasant: n = 85 years). KA was the coldest and wettest site, and MP was the warmest and received the most solar radiation. DL was relatively warmer and drier, whereas SL was colder and drier. Monthly and annual precipitation patterns were not necessarily parallel. For example, although MP received more precipitation than DL over the entire year, DL received more precipitation than MP during the peak of the growing season, from late April through late August (Figure 2).

2.3. Model Structure

[15] The PnET family of forest ecosystem models integrates algorithms that estimate atmospheric environment, canopy photosynthesis, phenology, water balance, and allocation routines, which distribute annual carbon gain among foliage, wood, and roots. Monthly climate inputs constrain carbon gain through a multilayered canopy submodel, which estimates photosynthesis, respiration, and evapotranspiration and calculates a C balance for each layer [Aber *et al.*, 1995]. In addition, PnET-CN adds algorithms for litter production, decomposition, root growth and maintenance respiration, soil CO₂ flux, and N mineralization, allowing C to interact with N in several submodels. These algorithms allow system N pools, which drive photosynthetic potential through foliar N, to adjust dynamically in response to litter volume, quality, and decomposition rates [Aber *et al.*, 1997]. The canopy submodel of PnET is built around a group of physiological relationships between foliar N, photosynthetic capacity, vertical scaling of leaf mass area, and leaf life span [Aber *et al.*, 1995, 1996; Ellsworth and Reich, 1993; Gower *et al.*, 1993; Reich *et al.*, 1998a]. A heat-sum algorithm controls phenology, with the model adding foliage mass when growing degree day

Table 1. Annual Climate Means^a

Climate Variable	DL	SL	KA	MP
MAT (°C)	4.14	1.47	0.82	8.16
MApar (μmol m ⁻² s ⁻¹)	619.82	517.79	540.21	657.24
MAP (cm)	67.67	73.75	83.01	74.59

^aMeans calculated from the available climate record from the Midwest Regional Climate Center and the Canadian National Climate Data and Information Archive (SW: n = 107 years; NW: n = 71 years; NE: n = 72 years; and SE: n = 85 years). DL, Detroit Lakes, Minnesota—southwest; KA, Kapuskasing, Ontario, Canada—northeast; MAP, mean annual precipitation; MApar, mean annual photosynthetically active radiation; MAT, mean annual temperature; MP, Mount Pleasant, Michigan—southeast; SL, Sioux Lookout, Ontario, Canada—northwest.

Table 2. Site Parameters^a

Parameter	Description	DL	SL	KA	MP
Lat	Latitude (°)	46.83	50.12	49.12	43.57
WHC	Soil water holding capacity (cm of available H ₂ O within rooting profile)	12	12	12	12
Water stress ^b	Toggle	1	1	1	1
Snow pack	Snow depth (cm)	22	72	82	13
NH4dep	NH ₄ deposition (g N m ² yr ⁻¹)	0.0151	0.0151	0.0151	0.0151
NO3dep	NO ₃ deposition (g N m ² yr ⁻¹)	0.0165	0.0165	0.0165	0.0165

^aDL, Detroit Lakes, Minnesota—southwest; KA, Kapuskasing, Ontario, Canada—northeast; MP, Mount Pleasant, Michigan—southeast; SL, Sioux Lookout, Ontario, Canada—northwest. For additional discussion of parameter definitions, see Aber *et al.* [1995, 1997] and Ollinger *et al.* [2002].

^bWhen set to 0, the toggle turns off the effects of water stress on gross primary production calculations. In effect, removes the constraints of a less than optimum water supply.

Table 3. Vegetation Parameters for Aspen, Spruce, and Pine^a

Parameter	Description	Aspen	Spruce	Pine
AmaxA	Intercept (A) and slope (B) for foliar N	-46	5.3	5.3
AmaxB	Photosynthesis relationship ($\mu\text{mol CO}_2 \text{ m}^{-2} \text{ leaf s}^{-1}$)	71.9	21.5	21.5
AmaxFrac	Amax as fraction of early morning instantaneous rate	0.75	0.75	0.75
BaseFolRespFrac ^b	Respiration as fraction of max photosynthesis	0.1	0.1	0.1
CFracBiomass	Carbon fraction of biomass	0.45	0.45	0.45
DVPD1	Coefficients for power function which convert	0.05	0.05	0.05
DVPD2	Vapor pressure deficit to fractional loss in photosynthesis	2	2	2
GDDFolStart	Growing degree day onset of foliage production	100	300	900
GDDFolEnd	Growing degree day end of foliage production	900	1400	1600
HalfSat	Half saturation light level ($\mu\text{mol CO}_2 \text{ m}^{-2} \text{ s}^{-1}$)	200	200	200
PsnTMin	Minimum temperature for photosynthesis ($^{\circ}\text{C}$)	4	0	4
PsnTOpt	Optimum temperature for photosynthesis ($^{\circ}\text{C}$)	24	20	24
RespQ10 ^a	Q_{10} of respiration	2	2	2
SLWdel	Change in specific leaf weight as foliar mass increases above ($\text{g m}^{-2} \text{ g}^{-1}$)	0.2	0	0
SLWmax ^b	Specific leaf weight at canopy top (g m^{-2})	84	235	235
K	Canopy light attenuation constant	0.45	0.5	0.5
FolNCon ^b	Start values for foliar [N]	2.47	0.95	1.22
FolRelGrowMax	Maximum relative foliage growth rate (yr^{-1})	0.75	0.3	0.75
RootAllocA	Intercept (A) and slope (B) of the fine root foliage relationship	0	0	0
RootAllocB		2	2	
RootMRespFrac	Fine root maintenance respiration-to-biomass production ratio	1	1	1
PlantCReserveFrac	Plant C fraction reserved after bud allocation	0.25	0.25	0.25
MinWoodFolRatio	Wood:foliage C allocation minimum	1.5	1.25	1.25
WUEConst	Water use efficiency as a function of vapor pressure deficit equation constant	10.9	10.9	10.9
PrecIntFrac	Fraction of precipitation intercepted and evaporated	0.11	0.15	0.15
FastFlowFrac	Fraction of H_2O lost to drainage	0.1	0.1	0.1
f	Soil H_2O release parameter	0.04	0.04	0.04
SoilRespA	Intercept (A) and slope (B) in relationship of mean temperature and soil respiration ($\text{g C m}^{-2} \text{ mo}^{-1}$)	27.46	27.46	27.46
SoilRespB		0.0684	0.0684	0.0684
WoodTurnOver	Live wood mortality fraction (yr^{-1})	0.025	0.025	0.025
RootTurnOverA	Quadratic coefficients for fine root turnover (fraction yr^{-1}) as a function of annual N mineralization	0.789	0.789	0.789
RootTurnOverB		0.191	0.191	0.191
RootTurnOverC		0.0211	0.0211	0.0211
FolReten ^c	Foliage retention time (yr)	1	5.42	4
Kho (Ksom)	Decomposition constant for soil organic matter (yr^{-1})	0.075	0.075	0.075
NImmobA	Coefficients of fraction of mineralized N remobilized as function of soil organic matter C:N	151	151	151
NImmobB		-35	-35	-35
MaxNStore	Max N content in mobile plant pool (g m^{-2})	80	80	80
GDDWoodStart	Wood production onset (growing degree days)	100	300	900
GDDWoodEnd	End of wood production (growing degree days)	900	1400	1600
FolNConRange	Max fractional increase in [N]	0.6	0.6	0.5
FLPctN	Minimum [N] in foliar litter (%)	0.009	0.0035	0.004
RLPctN	Minimum [N] in root litter (%)	0.012	0.011	0.012
WLPctN	Minimum [N] in wood litter (%)	0.002	0.002	0.002
WoodLitLossRate	Fraction transfer from dead wood to soil organic matter (yr^{-1})	0.1	0.1	0.1
WoodLitLoss	Fractional loss of C mass in wood decomposition	0.8	0.8	0.8

^aFor additional discussion of parameter definitions, see *Aber et al.* [1995, 1997] and *Ollinger et al.* [2002].

^bIndicates a parameter for which RA algorithms were substituted in the acclimation simulations.

^cEstimated from *Reich et al.* [1998b, 1999].

conditions are met. Canopy size and leaf off are controlled by light attenuation and each layer's subsequent C balance. This results in the model trimming, from the subsequent year's canopy mass, layers that do not retain a positive C balance at the end of the year [*Aber et al.*, 1995]. The effects of CO_2 on photosynthesis follow *Ollinger et al.* [2002], who added a Michaelis–Menten function fit to normalized $A-C_i$ curves and incorporated a variable C_i/C_a ratio that varies with foliar N, along with a stomatal conductance response, which adjusts conductance with changes in photosynthesis and C_a and C_i . In application, these algorithms result in positive feedback between CO_2 and photosynthetic capacity, and a negative feedback between CO_2 and transpiration, or in other words, rising atmospheric CO_2 increases photosynthesis and reduces water loss through transpiration.

[16] Because evidence to date (see previous section) suggests that only by combining the temperature-sensitive Q_{10} and acclimating basal rate could we actually simulate RA, we substituted both algorithms simultaneously for PnET-CN's fixed Q_{10} and fixed basal respiration parameters. In addition, because of uncertainty about the ubiquity and form of belowground soil acclimation, we do not incorporate this effect. The individual effects of temperature-sensitive Q_{10} and sliding basal respiration algorithms have been presented elsewhere (see *Wythers et al.* [2005] for additional detail), and in any case, as both are likely fundamental aspects of basic biology and required to adequately represent long-term thermal acclimation of respiration, modeling both together seems to be the most parsimonious approach. The

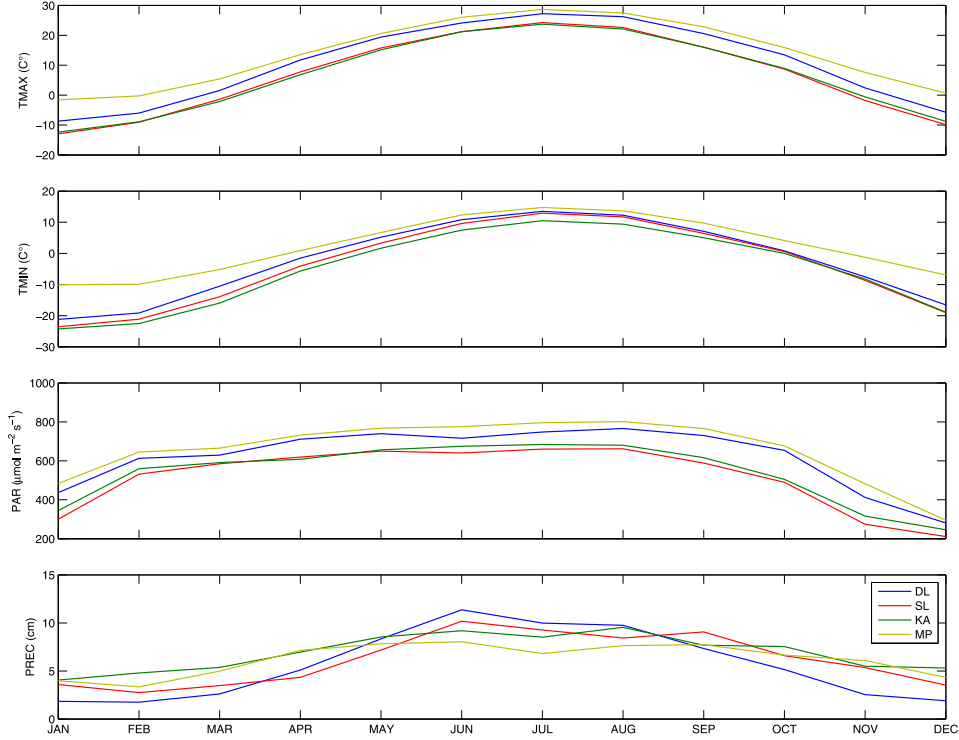


Figure 2. Monthly climate means for Detroit Lakes, Minnesota—southwest (DL); Sioux Lookout, Ontario, Canada—northwest (SL); Kapuskasing, Ontario, Canada—northeast (KA); and Mount Pleasant, Michigan—southeast (MP). Means calculated from the available climate record from the Midwest Regional Climate Center and the Canadian National Climate Data and Information Archive. Data for t_{max} ($^{\circ}\text{C}$) and t_{min} ($^{\circ}\text{C}$) represent monthly means, precipitation (cm) are totals for the month, and PAR values are calculated for the middle day of each month and converted to $\mu\text{mol m}^{-2} \text{day}^{-1}$, then divided by day length, resulting in $\mu\text{mol m}^{-2} \text{s}^{-1}$ (DL: $n = 107$ years; SL: $n = 71$ years; KA: $n = 72$ years; and MP: $n = 85$ years).

temperature-sensitive Q_{10} of respiration is from *Tjoelker et al.* [2001]:

$$\text{Temperature sensitive } Q_{10} = 3.22 - 0.046T, \quad (2)$$

where temperature-sensitive Q_{10} is the Q_{10} of foliar respiration and T is the midpoint between the measurement temperature and the reference temperature ($^{\circ}\text{C}$). As implemented in PnET-CN, the midpoint is defined as the average of the temperature at each time-step and photosynthetic optimum parameter for each vegetation type. Basal respiration is defined as follows:

$$\begin{aligned} \text{Long-term leaf respiration acclimation} \\ = Amax \cdot [0.14 - 0.002T], \end{aligned} \quad (3)$$

where long-term leaf RA is dark respiration ($\mu\text{mol CO}_2 \text{ m}^{-2} \text{ leaf s}^{-1}$), $Amax$ is the maximum photosynthetic rate ($\mu\text{mol CO}_2 \text{ m}^{-2} \text{ leaf s}^{-1}$), and T is the average temperature ($^{\circ}\text{C}$). Equations 2 and 3 replace PnET-CN's $BaseFolRespFrac$ and Q_{10} parameters, respectively. Taken together, equations 2 and 3 alter PnET-CN's fixed parameter respiration algorithm from:

$$R = [BaseFolRespFrac \cdot Amax] \cdot Q_{10}^{\left[\frac{T - T_{ref}}{10}\right]}, \quad (4)$$

where R is foliar respiration, $BaseFolRespFrac$ is 0.1, Q_{10} is 2, $Amax$ is the maximum photosynthetic rate ($\mu\text{mol CO}_2 \text{ m}^{-2}$

leaf s^{-1}), T is average temperature ($^{\circ}\text{C}$), and T_{ref} is the optimum temperature for photosynthesis ($^{\circ}\text{C}$), to:

$$R = [[0.14 - 0.002T] \cdot Amax] \cdot \left[3.22 - 0.046 \left[\frac{T + T_{ref}}{2} \right]^{\left[\frac{T - T_{ref}}{10} \right]} \right], \quad (5)$$

where R is foliar respiration, T is average temperature ($^{\circ}\text{C}$), $Amax$ is the maximum photosynthetic rate ($\mu\text{mol CO}_2 \text{ m}^{-2} \text{ leaf s}^{-1}$), and T_{ref} is the optimum temperature for photosynthesis ($^{\circ}\text{C}$). The combined impact of equations 2 and 3 on respiration is illustrated in Figure 3. MATLAB code is available upon request.

2.4. Scenarios

[17] We ran each PnET-CN scenario within a Monte Carlo multivariate time series algorithm following *Wilks* [2006]. The Monte Carlo algorithm performed 500 iterations using monthly climate data for each simulation to plot mean model output with confidence intervals ($p = 0.01$). The climate data were stochastically drawn from the multivariate normal distribution of historic monthly means and covariances of maximum and minimum temperature, precipitation, and solar radiation (PAR). The Monte Carlo wrapper allowed us to project future output means from historically variable climate drivers. We ran all iterations for 1000 years to stabilize C and N pools before implementing the climate change

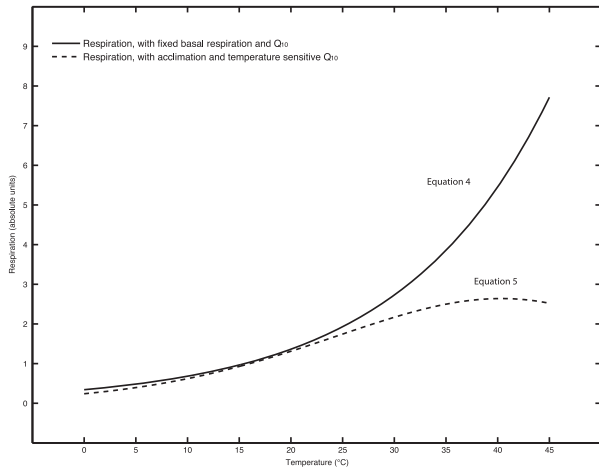


Figure 3. Schematic illustrating the effects of RA on foliar respiration. Foliar respiration with fixed basal respiration and fixed Q_{10} are represented by PnET-CN’s original respiration algorithms (equation 4) using parameter values of 0.1 for BasalFolRespFrac and 2.0 for Q_{10} (solid line). Foliar respiration with acclimation and a temperature-sensitive Q_{10} (equation 5) represents the effects of incorporating equations 2 and 3 into PnET-CN modeling structure (dashed line).

scenarios. To test the effects of global change drives, we used climate scenarios for ambient (i.e., historic) conditions, rising $[\text{CO}_2]$, warming, and rising $[\text{CO}_2]$ with warming. The ambient scenario used historic $[\text{CO}_2]$ levels of 280 ppm until year 1800 and then increased atmospheric $[\text{CO}_2]$ following the Keeling curve [Keeling and Whorf, 1995], reaching 380 ppm by year 2000, at which point we held $[\text{CO}_2]$ at 380 ppm for the duration of the simulation. The rising $[\text{CO}_2]$ scenario used the same CO_2 ramp described earlier, but in addition, the algorithm continued to increase $[\text{CO}_2]$, reaching 600 ppm by year 2100. The temperature ramp reproduced the Hadley A2a scenario, which resulted in a linear ramp achieving a 6°C increase at year 2100, relative to historic means. Lastly, we applied the CO_2 and warming simulations simultaneously.

[18] To quantify the impact of the RA algorithms, we ran the model with the original static respiration parameters for each scenario, and then reran the model in RA mode, substituting both the single temperature-sensitive Q_{10} and sliding long-term leaf RA algorithms for fixed respiration parameters. We examined the output means from the 500 iterations from each scenario for NPP, foliage mass, foliar N, and ecosystem respiration to gross primary production ratios (RE:GPP) for 150 years (years 2000–2150). To compare the effects on model output of RA algorithms with eddy flux data, we calculated ecosystem respiration/gross primary production ratios from relevant Ameriflux Network sites. Ameriflux sites were chosen based on proximity to study region, cover type, and data availability.

3. Results

[19] RA algorithms altered NPP response to rising $[\text{CO}_2]$ and warming, with associated changes in foliage mass and foliar N for all sites and forest types. However, the effects of RA algorithms on the magnitude and relative trajectory

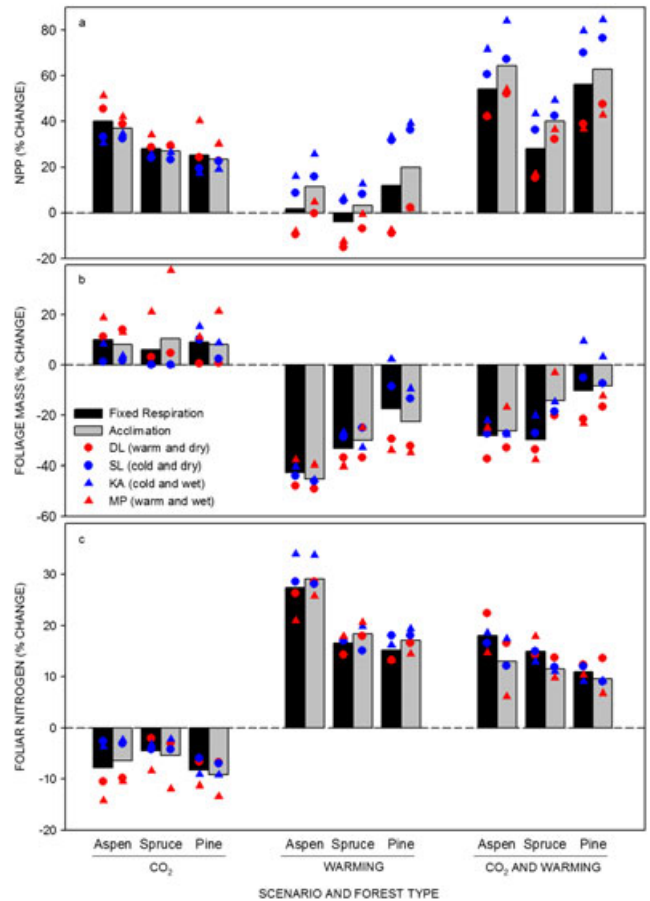


Figure 4. RA effects, at year 2100, as percentage change (acclimation: gray bars; fixed respiration parameters: black bars) on NPP (a), foliage mass (b) and foliar nitrogen (c), under three global change scenarios (rising $[\text{CO}_2]$, warming, and rising $[\text{CO}_2]$ with warming), for three forest types (aspen, spruce, and pine) at four sites (Detroit Lakes, Minn.: southwest (DL)—red circles; Sioux Lookout, Ontario, Canada: northwest (SL)—blue circles; Kapuskasing, Ontario, Canada: northeast (KA)—blue triangles; and Mount Pleasant, Mich.: southeast (MP)—red triangles).

of the NPP response, as well as the interactions between rising $[\text{CO}_2]$ and warming, varied by site and by forest type (Figures 4 and 5a). The effects of including RA algorithms on NPP in the rising $[\text{CO}_2]$ scenarios were modest and varied somewhat across sites and vegetation types. In contrast, including RA algorithms in the warming scenarios led to much greater warming enhancement of NPP, with or without rising $[\text{CO}_2]$.

3.1. NPP

3.1.1. Ambient

[20] Under the ambient scenario, incorporation of RA algorithms resulted in $\approx 25\%$ increases in NPP (average for all sites) compared to model runs with fixed respiration parameters (see Table S1 in the supporting information). Incorporating RA into the ambient scenario had a greater effect on NPP in the spruce and pine forest types (26–27% increases) than in aspen (a 19% increase). Increasing NPP in model runs that included RA were primarily due to lower

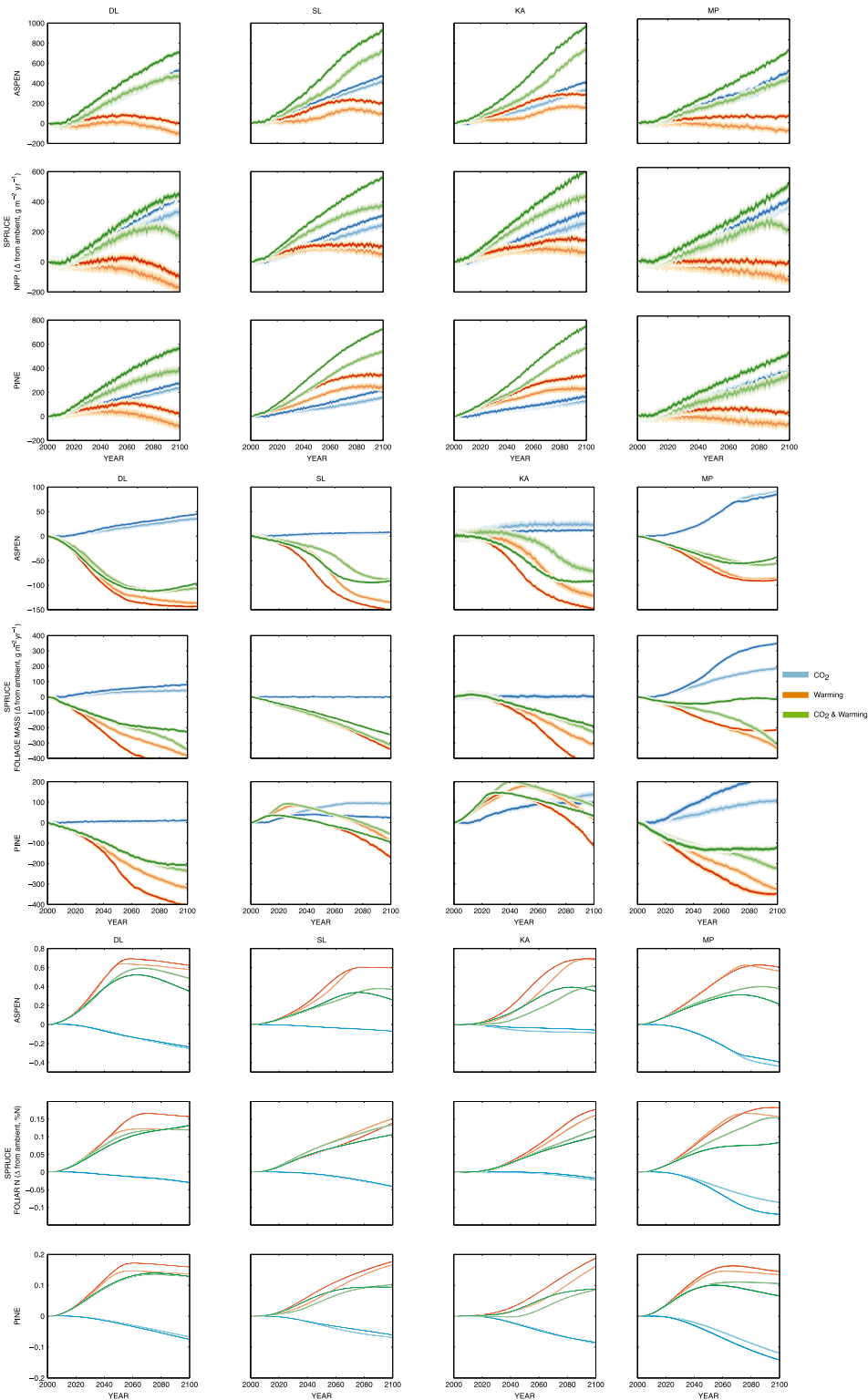


Figure 5. Differences from ambient climate (no CO₂ ramp or warming). Positive values are increases from ambient climate, whereas negative values are decreases from ambient climate. Confidence intervals are plotted in terms of probability ($p = 0.01$) from 500 model iterations with random climate draws using historic covariance relationships among t_{max} , t_{min} , PAR, and precipitation. Model output from years 2000 to 2100 represents forest type and site combinations for aspen, spruce, and pine from Detroit Lakes, Minnesota: southwest (DL); Sioux Lookout, Ontario, Canada: northwest (SL); Kapuskasing, Ontario, Canada: northeast (KA); and Mount Pleasant, Michigan: southeast (MP). Rising [CO₂] (blue), warming (red), and rising [CO₂] with warming (green). Darker colors represent runs performed with RA algorithms; lighter colors represent fixed respiration parameter runs for (a) NPP ($\text{g biomass m}^{-2} \text{yr}^{-1}$), (b) foliage mass (g m^{-2}), and (c) foliar N (%).

annual respiration but partially due to greater GPP due to increases in total canopy foliage mass (foliage mass hereafter), which ranged from as little as 5% across all forest types at the warmest site (SE) to as much as 17% at the coldest site (NE). Similarly, the lower impact of RA on aspen NPP was due to a smaller stimulation of foliage mass (6%) in aspen than in the two coniferous forest types (12–17%; see Table S2 in the supporting information). Incorporation of RA algorithms into the model increased NPP under ambient conditions, as shown previously [Atkin *et al.*, 2008; King *et al.*, 2006; Wythers *et al.*, 2005]; however, the focus of this article goes beyond this, in considering whether RA influences the response of NPP to global change drivers. In the following sections we focus on whether the change in NPP under several global change scenarios would be larger, smaller, or unchanged by incorporation of RA into the model. If responses are markedly different with RA versus without RA, it suggests additional care must be taken in interpreting even relative changes in NPP from prior models of NPP response to global change that were made with fixed respiration parameters.

3.1.2. Rising [CO₂]

[21] Across forest types and sites, rising [CO₂] resulted in large increases (e.g., 20–40% by 2100) in NPP, and RA had modest but inconsistent impact on those increases. At year 2100, averaged across vegetation types, incorporating RA algorithms into the rising [CO₂] scenario resulted in slightly smaller NPP increases due to rising [CO₂] at the two warmer sites but had little to no impact at the cooler sites (Figures 4a and 5a). Independent of the issue of RA effects on C balance, the strong and persistent [CO₂] fertilization of NPP effect suggests that, given the model logic of PNET-CN, long-term rising [CO₂] will not result in a down-regulation of soil N availability (see also section 3.1.3). Thus, there is no support in our results for the progressive N limitation hypothesis [Luo *et al.*, 2004].

3.1.3. Warming

[22] Across forest types, the model with fixed respiration parameters predicted that the warming scenario would result in increased NPP in the cold sites and decreased NPP at the warm sites (at 2100). Including RA in the model made all of the responses more positive for all forest types and sites. Incorporating RA algorithms into the warming scenario resulted in NPP increases, at year 2100, 3% to 13% larger than NPP increases due to fixed parameters. Spruce was least positively affected by warming and exhibited the smallest increase in NPP response when RA algorithms were used.

3.1.4. Rising [CO₂] and Warming

[23] Across forest types and sites, the combination of rising [CO₂] with warming had a large positive impact on NPP that was generally greater than additive, when compared to the impacts of each global change driver alone. The NPP response was more stimulated at the cool than warm sites, and in aspen and pine compared with spruce. These increases in NPP due to combined rising [CO₂] and warming were all larger (5–19%) with RA algorithms than with fixed parameters. The RA algorithms had somewhat different impacts depending on site and forest type. The impact of RA on spruce NPP response to the joint effects of rising [CO₂] and warming were more enhanced at the

warm sites than for the other species or for spruce at cool sites. This contrasts with modest impacts of RA on spruce for rising [CO₂] or warming alone.

3.2. Foliage Mass

3.2.1. Rising [CO₂]

[24] Across forest types and sites, rising [CO₂] resulted in ≈10% increases (by 2100) in foliage mass, and RA had varying impact on those increases depending on site and species. Incorporating RA algorithms resulted in foliage mass increases due to rising [CO₂] that ranged (at 2100) from 8% less to as much as 17% more than with fixed respiration parameters. Averaged across forest types, RA algorithms resulted in smaller foliage mass increases, due to rising [CO₂], at the two cooler than the warmer sites. The largest impact of including RA algorithms occurred in the two conifers at the warmest site (17% and 10% increases in foliage mass in spruce and pine, respectively, at SE; Figures 4b and 5b).

3.2.2. Warming

[25] Across forest types and sites, simulations using both fixed respiration parameters and simulations using RA algorithms predicted that warming would result in decreased foliage mass, with aspen the most sensitive and pine the least, although pine foliage mass at the cold sites showed a modest increase for the first few years of the simulation before starting to decrease beyond year 2050 (Figure 5b). Including RA in the model had mixed impacts on these predicted decreases. RA algorithms resulted in greater (warming-induced) decreases in aspen and pine, but smaller decreases in spruce with the exception of the NE site. For pine in particular, reductions in foliage mass due to warming were particularly large at the two southern sites.

3.2.3. Rising [CO₂] and Warming

[26] Foliage mass responses to rising [CO₂] and warming were roughly additive compared to the responses to either rising [CO₂] or warming alone. The general tendency toward decreases in foliage mass due to the combined effects of rising [CO₂] and warming tended to be smaller with RA algorithms than with fixed parameters. This impact of incorporation of RA into the model was most dramatic in spruce (16% less reduced) and larger at warm than cool sites.

[27] Because the amount of foliage mass displayed each year is limited by canopy layers with a positive C balance from the previous year [Aber *et al.*, 1995], C conserved by RA algorithms tends to push “marginal” canopy layers into positive C balance status, retaining the foliage mass of those layers, in the subsequent years’ canopy. The more canopy layers that fall into this “tipping point” C balance status, the more canopy layers that are likely to be conserved by RA algorithms. In addition, RA influences on canopy size affect C gain via feedbacks through the CO₂ response, which scales photosynthesis with C_i/C_a ratio and reduced stomatal conductance [Ollinger *et al.*, 2002]. Therefore, forest type-site combinations nearer their canopy’s physiological climate limits are where the effects of RA algorithms are largest.

3.3. Foliar N

3.3.1. Rising [CO₂]

[28] The model predicted decreased foliar N concentrations, across all forest types and sites, due to the effects of rising [CO₂] (see Table S3 in the supporting information). The warm sites generally displayed larger CO₂-induced decreases than the cold sites, with the exception of the spruce. Including RA algorithms had minor, and inconsistent, impacts on those decreases, causing slightly smaller decreases in aspen at the MP site, and slightly larger decreases in spruce and pine at the warmest (MP) site (Figure 5c). Overall, the effects of RA algorithms in the rising [CO₂] scenario were small, ranging from 4% less to 4% more than the effects of rising [CO₂] using fixed respiration parameters (Figure 4c).

3.3.2. Warming

[29] Across all sites and forest types, simulations using both fixed respiration parameters and RA algorithms predicted increased foliar N due to warming. Including RA algorithms in the warming scenarios consistently resulted in larger foliar N increases, especially at the warm sites. However, the effects of RA algorithms on foliar N increases were small. The largest increase was in aspen at the warmest site (SE, 5%), but when averaged across forest types, including RA algorithms resulted in a less than 3% increase at any site.

3.3.3. Rising [CO₂] and Warming

[30] The combination of rising [CO₂] with warming, across all forest types and sites, had a positive impact on foliar N, which was generally additive in aspen and spruce, when compared to the impacts of each global change driver

alone, but slightly larger than additive in pine. Averaged across sites, incorporating RA algorithms into the combined rising [CO₂] and warming scenarios resulted in smaller foliar N increases (1–5% less) than those under fixed respiration parameters. RA algorithms had somewhat variable impacts, depending on site and forest type. Foliar N increases due to rising [CO₂] and warming were most reduced by RA algorithms in aspen and spruce at the warmest site (SE, –9% and –8%, respectively). This result contrasts with more modest impacts of RA on aspen and spruce at MP in rising [CO₂] or warming scenarios individually. The impacts of RA on foliar N response to global change drivers were primarily due to RA effects on foliage mass, which was indirectly related to N mineralization.

3.4. NEE

[31] Impacts of incorporating RA algorithms resulted in similar impacts on modeled NEE responses to CO₂ and warming (see supporting information; Figure 2) as on modeled NPP responses (Figure 5a). The percentage changes in NEE were often large, which is not surprising given that NEE can be very near zero. However, the patterns of impacts of considering RA in models of NEE very closely mirror those for NPP (compare supporting information to Figures 1 and 4a). As this model modifies foliar respiration but not soil respiration, it is not surprising that impacts on NPP and NEE vary in parallel.

3.5. RE:GPP

[32] Eddy flux data from three deciduous broadleaf forests in our study region indicated a mean RE:GPP of 0.38 (Table 4). By comparison, RE:GPP from our PnET simulations averaged 0.41 for deciduous hardwoods when RA is

Table 4. Eddy Flux, Ecosystem Respiration: Gross Primary Production Ratios^a

Site ^b	Latitude, Longitude (°)	Description ^c	Years	\bar{x}	Range
UMBS	45.56, –84.71	Deciduous broadleaf	2004–2011	0.42	0.35–0.45
WCr	45.80, –90.08	Deciduous broadleaf	2000–2006	0.35	0.29–0.42
Hol1	45.20, –68.74	Evergreen needleleaf	1996–2008	0.42	0.37–0.45
Hal1	42.54, –72.17	Deciduous broadleaf	1992–2010	0.37	0.23–0.51
Dk3	35.98, –79.09	Evergreen needleleaf	1998–2005	0.37	0.29–0.43

^aSummary statistics calculated for May through September each year.

^bDk3, Duke Forest, Durham, North Carolina; Hal1, Harvard Forest, Petersham, Massachusetts; Hol1, Howland, Orono, Maine; UMBS, University of Michigan Biological Station, Pelston, Michigan; WCr, Willow Creek, Woodruff, Wisconsin.

^cDominant vegetation: UMBS, bigtooth and trembling aspen; WCr, sugar maple, basswood, and green ash; Hol1, spruce, fir, and hemlock; Hal1, red oak and red maple; and Dk3, loblolly pine.

Table 5. PnET-CN, Ecosystem Respiration: Gross Primary Production Ratios^a

Site ^b	Aspen		Spruce		Pine	
	Fixed	ra	Fixed	ra	Fixed	ra
DL	0.50 (0.51)	0.41 (0.39)	0.53 (0.55)	0.45 (0.46)	0.53 (0.55)	0.45 (0.45)
KA	0.47 (0.48)	0.41 (0.38)	0.52 (0.53)	0.44 (0.45)	0.51 (0.52)	0.45 (0.44)
MP	0.50 (0.53)	0.41 (0.39)	0.53 (0.54)	0.42 (0.46)	0.55 (0.57)	0.44 (0.46)
SL	0.48 (0.48)	0.41 (0.38)	0.52 (0.53)	0.44 (0.45)	0.51 (0.52)	0.46 (0.44)

^aRE:GPP ratios are means, calculated for May through September each year, from all climate iterations from years 2012 and 2100 (in parentheses) for model runs with fixed respiration parameters and respiration acclimation (ra).

^bDL, Detroit Lakes, Minnesota—southwest; KA, Kapuskasing, Ontario, Canada—northeast; MP, Mount Pleasant, Michigan—southeast; SL, Sioux Lookout, Ontario, Canada—northwest.

incorporated into the model and averaged 0.50 with fixed respiration parameters (Table 5). Eddy flux data from two evergreen needleleaf forests indicated mean RE:GPP of 0.40; our PnET results averaged 0.44 with RA and 0.53 without RA.

4. Discussion

[33] We sought to quantify the magnitude and direction in which RA influences how NPP, foliage mass, and foliar N respond to global change drivers. Our results suggest that RA algorithms increase response of NPP to warming (both with and without rising CO_2), whereas RA algorithms have less consistent impacts on foliage mass and foliar N responses to warming. This suggests impacts of improved respiration algorithms on model output are largely on direct temperature impacts rather than through indirect effects on canopy C and N pools or concentrations, and that RA will contribute to the ability of cold temperate and boreal forests to achieve greater NPP under higher temperatures and longer growing seasons.

[34] The differences in RA effects among sites were due to interactions among forest type and site characteristics, and the influence of the two substituted respiration algorithms on different regions of the respiration–temperature response curve. Because long-term leaf RA (equation 3) conserves C at the warmer end of the temperature response curve, and the temperature-sensitive Q_{10} (equation 2) conserves C at the cooler end of the response curve [Wythers *et al.*, 2005], the combined effects of long-term leaf RA and temperature-sensitive Q_{10} , relative to fixed respiration parameters (Figure 3), contrasts with the effects of using long-term leaf RA only, where at lower temperatures, C losses through respiration are increased relative to fixed respiration parameters [Wythers *et al.*, 2005; Atkin *et al.*, 2008]. These distinct effects on respiration, due to the two components of the RA algorithms, combined with canopy trait differences of the three forest types to give us the results that we examine in greater detail below.

[35] In the following sections, we examine temporal trends; the relationships among NPP, foliage mass, and foliar N responses to RA algorithms; the possible mechanistic explanations; and how these compare to both empirical results and theoretical thinking about these issues.

4.1. Comparison of Experimental Evidence of CO_2 and Warming Effects

[36] Free air carbon dioxide enrichment experiments provide important evidence of effects of rising CO_2 on natural plant communities. Our results are largely consistent with recent meta-analyses of free air carbon dioxide enrichment data that show tree responses to elevated CO_2 (475–600 ppm) comparable to our simulated CO_2 at year 2100 (600 ppm). For example, increasing CO_2 has been shown to have a positive effect on photosynthesis and foliage mass, while having a negative effect on foliar N [Ainsworth and Long, 2005; Ainsworth and Rogers, 2007; Ainsworth *et al.*, 2007]. Similarly, we observed a range of responses in NPP, foliage mass, and foliar N among our modeled sites forest type combinations, which agree with previously reported confidence intervals [Ainsworth and

Long, 2005; Ainsworth *et al.*, 2007]. From years 2000 to 2100, rising CO_2 affected a nearly linear and continuous increase in NPP (Figure 5). The rate of increase, however, varied among forest type-site combinations, with the largest differences relative to ambient climate occurring at the warm sites and in aspen. Foliage mass response to rising CO_2 showed similar site-forest type specificity. The largest differences were observed at DL (all forest types), KA (pine), and SL (pine), when foliage mass increased rapidly in the first 50 years, followed by a period of little or no change. This contrasts with other site-forest type combinations (e.g., spruce at the northern (colder) sites and pine at the southern (warmer) sites), where rising CO_2 had little or no effect on foliage mass. This supports the conclusion that for rising CO_2 alone, a saturation point for foliage mass will likely be reached sometime in the first half of the 21st century.

[37] From years 2000 to 2100, rising CO_2 reduced foliar N, in manner that most closely resembled a logarithmic decrease, relative to the ambient scenarios, and was consistent with empirical observations [Ainsworth and Long, 2005]. Given that foliar N is not directly influenced by rising CO_2 in PnET-CN, but instead is responding to short- and long-term feedbacks at plant and ecosystem scale of C and N pools and stocks and ratios, PnET-CN's predicted foliar N suggests that the model is performing well in these respects.

[38] To date, warming experiments have been performed with a variety of methods, including heat resistance cables, greenhouses, infrared lamps, chambers, and passive nighttime warming systems, although none at the scale of mature forests. Rustad *et al.* [2001] reported mean aboveground productivity increases of 19% in response to warming (0.3°C – 6°C), which were comparable to but more dramatic than our results of a mean 10% increase in NPP to warming at year 2100 (6.0°C). Rustad *et al.* [2001] also emphasized the need to understand the relative importance of factors such as successional status, site quality, land-use history, temperature, moisture, and so on in regulating ecosystem responses to warming. This conclusion is supported by our result that NPP response to temperature was heavily dependent on site–vegetation type combinations. For example, our simulations show NPP increasing from years 2000 to 2050. However, between years 2050 and 2100, NPP in our warming scenarios levels off and starts to decline. The exception to this trend is the warmest site (MP), where NPP in the warming treatment deviates very little from the ambient scenario.

[39] Predicted foliage mass tends to respond to warming with a sharp decline from 2000 to 2050, before slowing. However, pine foliage mass increases slightly, in response to warming at the two cold sites before falling below the ambient climate levels, when water becomes limiting at all four sites. Foliar N, on the other hand, increases rapidly in all forest type-site combinations in response to warming, before reaching the model's threshold for each forest type between years 2050 and 2100. In contrast to Beier *et al.* [2008], who reported an asymmetrical response (for European scrublands) to nighttime warming, with increasing C assimilation but decreasing N mineralization, our results suggest C assimilation and N cycling changed in parallel. In addition, Beier *et al.* [2008] reported similar responses of ecosystems from both cold and warm climate zones, where we observed

a more complex response to warming, with NPP tending to decline at our two warmer sites and increasing at our two cooler sites.

4.2. RA Effects with Rising [CO₂] and Warming

[40] RA algorithm effects on response of NPP to rising [CO₂] were essentially uniform from years 2000 to 2100. NPP estimates with RA displayed the same linear increase as the fixed parameter runs but were consistently higher. Foliage mass shifted in the positive direction due to RA algorithms and foliar N in a negative direction. Moreover, the foliage mass and foliar N responses to warming and rising [CO₂] with RA algorithms were more variable (relative to the fixed parameter responses) among forest type-site combinations than was NPP. Whereas *Leakey et al.* [2009] reported that rising [CO₂] increased carbon gain and productivity, and increased N and H₂O use efficiency in C₃ plants, despite down-regulation of Rubisco activity, others have shown that rising [CO₂] enhances the photosynthetic temperature response [*Alonso et al.*, 2009]. The NPP, foliage mass, and foliar N differences we report, relative to the effects of RA algorithms in ambient climate runs, were due in part to the interactions of (1) PnET-CN's CO₂ response algorithms, (2) PnET-CN's stomatal conductance algorithm, and (3) the tight linkage between Amax and foliar respiration rates.

[41] Including RA algorithms in the warming scenario resulted in greater NPP responses to warming at all sites and all vegetation types, relative to fixed parameter runs. In addition, the enhancement of NPP responses due to RA algorithms tended to increase over time relative to the fixed parameter results. However, the degree of increase varied among forest type-site combinations. For example, the enhancement of aspen NPP at KA (coldest site) due to RA increased up to year 2050, at which point no additional enhancement was seen, whereas in aspen at MP (warmest site), NPP enhancement due to RA over time increased throughout the entire simulation. RA's effect on the foliage mass response to warming was also variable among forest type-site combinations, and those effects varied over time. For example, there was little RA effect on foliage mass in spruce at MP (warmest site) until year 2060. However, in the simulation beyond year 2060, RA appeared to stabilize foliage mass losses in the warming scenario, whereas in the fixed parameter runs, foliage mass continued to decrease through time over the entire simulation period. In contrast, the effect of RA on spruce in the warming scenario at the coldest site (KA) was to enhance foliage mass losses, relative to fixed parameter runs. Likewise, the effect of RA in the warming scenario on foliar N varied over time and among forest type-site combinations, and by year 2100, tended to be larger at the warm sites. These particular interactions of RA algorithms with warming could be in part due to greater magnitude of impacts of down-regulation of respiration rates at higher temperatures, which are more common at the warmer sites. These results suggest that down-regulation of respiration would have a substantial impact on C balance and productivity, particularly in vegetation types with a lower photosynthetic temperature optimum, and on warm sites. These observations agree with the general findings that thermal acclimation is also associated with water stress in beech seedlings [*Rodriguez-Calcerrada et al.*, 2010] and Aleppo pine

[*Maseyk et al.*, 2008], and with foliar N variation reported in common garden-grown jack pine [*Tjoelker et al.*, 2008].

[42] NPP increases over time due to RA were greater than additive for some forest type-site combinations (relative to NPP increases over time in individual climate change driver simulations). In the combined climate change driver runs (rising [CO₂] and warming), the largest NPP enhancements due to RA were in spruce at the warm sites, where effects became quite pronounced by year 2100. However, in aspen at the cold sites, NPP enhancements due to RA increased over time through year 2060 before slowing to match those from fixed parameters. In the remaining forest type-site combinations, the general pattern of NPP enhancements due to RA increasing over time through the entire simulation was evident.

[43] Given that the combination of rising [CO₂] and warming is considered the most likely future scenario, model predictions for this scenario are most relevant and also most comparable to results and conclusions of *Atkin et al.* [2008] and *King et al.* [2006]. However, it is important to note that *King et al.* [2006] converted the temperature-sensitive Q_{10} component of our RA algorithms into an "equivalent temperature-dependent energy of activation (E_{aT})" for the GTEC model (see auxiliary text from *King et al.* [2006]), and *Atkin et al.* [2008] incorporated acclimation only into the JULES model to focus on the effects of acclimation alone, so it is important to ask how these differences in approach might have influenced model predictions. Although *Atkin et al.* [2008] acknowledged that their analysis could have differed had they taken a temperature-sensitive Q_{10} into account, our results support their general conclusion that it is important to account for thermal acclimation when modeling productivity. In our work, the inclusion of a temperature-sensitive Q_{10} appears to have important impacts on carbon balance at cooler sites (most likely higher latitudes and at altitude). In addition, our findings suggest that it is also important to consider the effects of RA within the context of specific forest type-site (climate zone) combinations. Our findings indicate that thermal environment and other site-specific characteristics act together with different vegetation types and produce unique productivity, foliage mass, and foliar N responses when RA algorithms are applied to rising [CO₂] and warming climate conditions. However, further work, particularly model comparisons to temperature-controlled experiments, is needed to add confidence to model results.

4.3. RE:GPP Comparisons

[44] RA algorithms reduced RE:GPP estimates from PnET-CN 7% across all sites and forest types for current climate (year 2012) and 9% under climate warming (year 2100). At all sites, results from PnET-CN with RA more closely approximated eddy covariance RE:GPP estimates than PnET-CN without RA. Whereas RA algorithms resulted in the largest RE:GPP decreases at MP (11% across all forest types) and in aspen (10% across all sites) relative to the other forest types, RE:GPP from all RA model runs were within the range of reported eddy flux RE:GPP values for their respective forest types; RE:GPP from PnET-CN runs without RA were not. Ecosystem respiration is quantified by a combination of measurement and modeling using data obtained by eddy covariance techniques, but is likely the best empirical approach available today. Thus, the general

agreement among PnET-CN's RE:GPP estimates with eddy covariance estimates, when RA algorithms are incorporated into the PnET model, helps to corroborate those estimates and contributes to greater confidence in the RA algorithms.

5. Conclusions

[45] With the exception of some warming-only climate change scenarios at the warmer sites, these model results suggest increases in NPP under all scenario combinations of forest types, sites, [CO₂], and warming. In particular, the model suggests a large increase in NPP in our study region under the most likely future conditions: increasing atmospheric [CO₂] coupled with climate warming. Incorporation of RA altered the magnitude and temporal trajectory of NPP increases and associated changes in foliage mass and foliar N. The impact of RA on NPP, foliage mass, and foliar N varied across sites, vegetation types, and global change scenarios. RA alone resulted in ≈25% upshift in NPP at year 2000. In rising [CO₂] simulations, RA resulted in smaller CO₂-induced NPP increases at warmer sites and slightly larger NPP increases in cooler sites. In warming conditions, RA resulted in substantially larger (or in some cases, less negative) NPP increases. In rising [CO₂] and warming conditions, RA resulted in larger NPP increases in all site-forest type combinations, and differences between fixed parameters and RA tended to increase over time. At year 2100, across all sites and vegetation types, NPP response to rising [CO₂] and warming was 9% greater with RA algorithms relative to fixed parameters, foliage mass was 11% greater with RA algorithms, and foliar N was 3% smaller when fixed parameters were replaced by RA algorithms. Impacts of RA on modeled responses of NEE to warming and CO₂ mirrored those of NPP. Our findings indicate that (1) the influence of RA on predicted changes in NPP with projected future [CO₂] and climate is often substantial and varies across forest types and sites; (2) incorporating RA into ecosystem models is important, particularly where a forest type may be persisting at its climate space limit; and finally, (3) the consequences of RA for ecosystem processes appear to increase over time.

[46] **Acknowledgments.** Funding for this research was provided by the United States Department of Agriculture, via joint venture agreement 09-JV-11244419-037, between the U. S. Forest Service and the University of Minnesota. Additional funding was supplied by the Wilderness Research Foundation and the Institute on the Environment, University of Minnesota. Any use of trade, product, or firm names is for descriptive purposes only and does not imply endorsement by the U. S. Government.

References

Aber, J. D., S. V. Ollinger, and C. T. Driscoll (1997), Modeling nitrogen saturation in forest ecosystems in response to land use and atmospheric deposition, *Ecol. Modell.*, *101*(1), 61–78.

Aber, J. D., S. V. Ollinger, C. A. Federer, P. B. Reich, M. L. Goulden, D. W. Kicklighter, J. M. Melillo, and R. G. Lathrop Jr. (1995), Predicting the effects of climate change on water yield and forest production in the northeastern United States, *Clim. Res.*, *5*(3), 207–222.

Aber, J. D., P. B. Reich, and M. L. Goulden (1996), Extrapolating leaf CO₂ exchange to the canopy: A generalized model of forest photosynthesis compared with measurements by eddy correlation, *Oecologia*, *106*(2), 257–265.

Ainsworth, E. A., and S. P. Long (2005), What have we learned from 15 years of free-air CO₂ enrichment (FACE)? A meta-analytic review of

the responses of photosynthesis, canopy properties and plant production to rising CO₂, *New Phytologist*, *165*(2), 351–372.

Ainsworth, E. A., and A. Rogers (2007), The response of photosynthesis and stomatal conductance to rising CO₂: Mechanisms and environmental interactions, *Plant Cell Environ.*, *30*(3), 258–270.

Ainsworth, E. A., M. S. Rosenberg, and W. Xianzhong (2007), Meta-analysis: The past, present and future, *New Phytologist*, *176*(4), 742–745.

Alonso, A., P. Perez, and R. Martinez-Carrasco (2009), Growth in elevated CO₂ enhances temperature response of photosynthesis in wheat, *Physiologia Plantarum*, *135*(2), 109–120.

Atkin, O. K., L. J. Atkinson, R. A. Fisher, C. D. Campbell, J. Zaragoza-Castells, J. W. Pitchford, F. I. Woodward, and V. Hurry (2008), Using temperature-dependent changes in leaf scaling relationships to quantitatively account for thermal acclimation of respiration in a coupled global climate-vegetation model, *Global Change Biol.*, *14*(11), 2709–2726.

Atkin, O. K., C. Holly, and M. C. Ball (2000), Acclimation of snow gum (*Eucalyptus pauciflora*) leaf respiration to seasonal and diurnal variations in temperature: The importance of changes in the capacity and temperature sensitivity of respiration, *Plant Cell Environ.*, *23*(1), 15–26.

Atkin, O. K., I. Scheurwater, and T. L. Pons (2006), High thermal acclimation potential of both photosynthesis and respiration in two lowland Plantago species in contrast to an alpine congener, *Global Change Biol.*, *12*(3), 500–515.

Atkin, O. K., D. Sherlock, A. H. Fitter, S. Jarvis, J. K. Hughes, C. Campbell, V. Hurry, and A. Hodge (2009), Temperature dependence of respiration in roots colonized by arbuscular mycorrhizal fungi, *New Phytologist*, *182*(1), 188–199.

Atkin, O. K., and M. G. Tjoelker (2003), Thermal acclimation and the dynamic response of plant respiration to temperature, *Trends Plant Sci.*, *8*(7), 343.

Beier, C., et al. (2008), Carbon and nitrogen cycles in European ecosystems respond differently to global warming, *Sci. Total Environ.*, *407*(1), 692–697.

Belehrádek, J. (1930), Temperature coefficients in biology, *Biol. Rev.*, *5*, 30–58.

Berry, J. A., and J. K. Raison (1981), Response of macrophytes to temperature, in *Encyclopedia of Plant Respiration, New Series*, edited by O. L. Lange, pp. 277–338, Springer, Berlin.

Bolstad, P. V., P. Reich, and T. Lee (2003), Rapid temperature acclimation of leaf respiration rates in *Quercus alba* and *Quercus rubra*, *Tree Physiol.*, *23*(14), 969–976.

Bradford, M. A., C. A. Davies, S. D. Frey, T. R. Maddox, J. M. Melillo, J. E. Mohan, J. F. Reynolds, K. K. Treseder, and M. D. Wallenstein (2008), Thermal adaptation of soil microbial respiration to elevated temperature, *Ecol. Lett.*, *11*(12), 1316–1327.

Christensen, J. H., et al. (2007), *Climate Change 2007: The Physical Science Basis: Contribution of Working Group I to the Fourth Assessment Report of the Intergovernmental Panel on Climate Change*, pp. 707–811, Cambridge University Press, Cambridge, U. K.

Coops, N. C., and R. H. Waring (2001), Estimating forest productivity in the eastern Siskiyou Mountains of southwestern Oregon using a satellite driven process model, 3-PGS, *Can. J. For. Res.*, *31*(1), 143.

Cramer, W., D. W. Kicklighter, A. Bondeau, B. M. Iii, G. Churkina, B. Nemry, A. Ruimy, A. L. Schloss, and the Participants of the Potsdam NPP Model Intercomparison (1999), Comparing global models of terrestrial net primary productivity (NPP): Overview and key results, *Global Change Biol.*, *5*, 1–15.

DeLucia, E. H., J. E. Drake, R. B. Thomas, and M. Gonzalez-Meler (2007), Forest carbon use efficiency: Is respiration a constant fraction of gross primary production? *Global Change Biol.*, *13*(6), 1157–1167.

Ellsworth, D. S., and P. B. Reich (1993), Canopy structure and vertical patterns of photosynthesis and related leaf traits in a deciduous forest, *Oecologia*, *96*(2), 169–178.

Fay, P. A. (2009), Precipitation variability and primary productivity in water-limited ecosystems: How plants “leverage” precipitation to “finance” growth, *New Phytologist*, *181*(1), 5–8.

Forward, D. F. (1960), Effect of temperature on respiration, in *Handbuch der Pflanzenphysiologie*, edited by W. Ruhland, pp. 234–258, Springer, Berlin.

Freligh, L. E., and P. B. Reich (2010), Will environmental changes reinforce the impact of global warming on the prairie-forest border of central North America?, *Front. Ecol. Environ.*, *8*(6), 371–378.

Gower, S. T., P. B. Reich, and Y. Son (1993), Canopy dynamics and aboveground production of five tree species with different leaf longevities, *Tree Physiol.*, *12*(4), 327–345.

Gunderson, C. A., R. J. Norby, and S. D. Wullschleger (2000), Acclimation of photosynthesis and respiration to simulated climatic warming in northern and southern populations of *Acer saccharum*: Laboratory and field evidence, *Tree Physiol.*, *20*, 87–96.

Gunn, S., and J. F. Farrar (1999), Effects of a 4 °C increase in temperature on partitioning of leaf area and dry mass, root respiration and carbohydrates, *Funct. Ecol.*, *13*, 12.

- Heisler-White, J. L., J. M. Blair, E. F. Kelly, K. Harmoney, and A. K. Knapp (2009), Contingent productivity responses to more extreme rainfall regimes across a grassland biome, *Global Change Biol.*, 15(12), 2894–2904.
- Heisler-White, J. L., A. K. Knapp, and E. F. Kelly (2008), Increasing precipitation event size increases aboveground net primary productivity in a semi-arid grassland, *Oecologia*, 158(1), 129–140.
- Intergovernmental Panel on Climate Change (2008), Scientific Assessment of the Effects of Global Change on the United States, National Science and Technology Council, Committee on Environment and Natural Resources, Washington, D. C.
- James, W. O. (1953), *Plant Respiration*, Clarendon Press, Oxford, U. K.
- Keeling, C. D., and T. P. Whorf (1995), Interannual extremes in the rate of rise of atmospheric carbon dioxide since 1980, *Nature*, 375(6533), 666.
- Kicklighter, D. W., A. Bondeau, A. L. Schloss, J. Kaduk, A. D. McGuire, and the Participants of the Potsdam NPP Model Intercomparison (1999), Comparing global models of terrestrial net primary productivity (NPP): Global pattern and differentiation by major biomes, *Global Change Biol.*, 5, 16–24.
- King, A. W., C. A. Gunderson, W. M. Post, D. J. Weston, and S. D. Wullschlegel (2006), Plant respiration in a warmer world, *Science*, 312(5773), 536–537.
- Larcher, W. (2003), *Physiological Plant Ecology: Ecophysiology and Stress Physiology of Functional Groups*, 4th ed., 120 pp., Springer-Verlag, Berlin.
- Leakey, A. D. B., E. A. Ainsworth, C. J. Bernacchi, A. Rogers, S. P. Long, and D. R. Ort (2009), Elevated CO₂ effects on plant carbon, nitrogen, and water relations: Six important lessons from FACE, *J. Exp. Bot.*, 60(10), 2859–2876.
- Le Quere, C., T. Takahashi, E. T. Buitenhuis, C. Roedenbeck, and S. C. Sutherland (2010), Impact of climate change and variability on the global oceanic sink of CO₂, *Global Biogeochem. Cycles*, 24(4), GB4007, doi:10.1029/2009GB003599.
- Lloyd, J. (1999), The CO₂ dependence of photosynthesis, plant growth responses to elevated CO₂ concentrations and their interaction with soil nutrient status, II. Temperate and boreal forest productivity and the combined effects of increasing CO₂ concentrations and increased nitrogen deposition at a global scale, *Funct. Ecol.*, 13(4), 439–459.
- Lou, Y., et al. (2008), Modeled interactive effects of precipitation, temperature, and CO₂ on ecosystem carbon and water dynamics in different climatic zones, *Global Change Biol.*, 14(9), 1986–1999.
- Lou, Y., et al. (2004), Progressive nitrogen limitation of ecosystem responses to rising atmospheric carbon dioxide, *BioScience*, 54(8), 731–739.
- Mahecha, M. D., et al. (2010), Global convergence in the temperature sensitivity of respiration at ecosystem level, *Science*, 329(5993), 838–840.
- Malcolm, G. M., J. C. Lopez-Gutierrez, R. T. Koide, and D. M. Eissenstat (2008), Acclimation to temperature and temperature sensitivity of metabolism by ectomycorrhizal fungi, *Global Change Biol.*, 14(5), 1169–1180.
- Maseyk, K., J. M. Grunzweig, E. Rotenberg, and D. A. N. Yakir (2008), Respiration acclimation contributes to high carbon-use efficiency in a seasonally dry pine forest, *Global Change Biol.*, 14(7), 1553–1567.
- Ollinger, S. V., J. D. Aber, P. B. Reich, and R. J. Freuder (2002), Interactive effects of nitrogen deposition, tropospheric ozone, elevated CO₂ and land use history on the carbon dynamics of northern hardwood forests, *Global Change Biol.*, 8(6), 545–562.
- Potter, C., J. Bubier, P. Crill, and P. Lafleur (2001), Ecosystem modeling of methane and carbon dioxide fluxes for boreal forest sites, *Can. J. For. Res.*, 31(2), 208.
- Reich, P. B. (2010), The carbon dioxide exchange, *Science*, 329(5993), 774–775.
- Reich, P. B., D. S. Ellsworth, and M. B. Walters (1998a), Leaf structure (specific leaf area) modulates photosynthesis-nitrogen relations: Evidence from within and across species and functional groups, *Funct. Ecol.*, 12(6), 948–958.
- Reich, P. B., D. S. Ellsworth, M. B. Walters, J. M. Vose, C. Gresham, J. C. Volin, and W. D. Bowman (1999), Generality of leaf trait relationships: A test across six biomes, *Ecology*, 80(6), 1955–1969.
- Reich, P. B., M. B. Walters, D. S. Ellsworth, J. M. Vose, J. C. Volin, C. Gresham, and W. D. Bowman (1998b), Relationships of leaf dark respiration to leaf nitrogen, specific leaf area and leaf life-span: a test across biomes and functional groups, *Oecologia*, 114(4), 471–482.
- Reich, P. B., M. B. Walters, M. G. Tjoelker, D. Vanderklein, and C. Buschena (1998c), Photosynthesis and respiration rates depend on leaf and root morphology and nitrogen concentration in nine boreal tree species differing in relative growth rate, *Funct. Ecol.*, 12, 395–405.
- Rodriguez-Calcerrada, J., O. K. Atkin, T. M. Robson, J. Zaragoza-Castells, L. Gil, and I. Aranda (2010), Thermal acclimation of leaf dark respiration of beech seedlings experiencing summer drought in high and low light environments, *Tree Physiol.*, 30, 214–224.
- Rustad, L. E., J. L. Campbell, G. M. Marion, R. J. Norby, M. J. Mitchell, A. E. Hartley, J. H. C. Cornelissen, J. Gurevitch, and N. Gcte (2001), A meta-analysis of the response of soil respiration, net nitrogen mineralization, and aboveground plant growth to experimental ecosystem warming, *Oecologia*, 126(4), 543–562.
- Sampson, D. A., I. A. Janssens, and R. Ceulemans (2006), Under-story contributions to stand level GPP using the process model SECRETS, *Agric. For. Meteorol.*, 139(1/2), 94–104.
- Schlesinger, W. H. (2005), *Biogeochemistry*, Elsevier, Amsterdam.
- Sitch, S., et al. (2008), Evaluation of the terrestrial carbon cycle, future plant geography and climate-carbon cycle feedbacks using five Dynamic Global Vegetation Models (DGVMs), *Global Change Biol.*, 14(9), 2015–2039.
- Tjoelker, M. G., J. Oleksyn, G. Lorenc-Plucinska, and P. B. Reich (2009), Acclimation of respiratory temperature responses in northern and southern populations of *Pinus banksiana*, *New Phytologist*, 181(1), 218–229.
- Tjoelker, M. G., J. Oleksyn, and P. B. Reich (1999a), Acclimation of respiration to temperature and CO₂ in seedlings of boreal tree species in relation to plant size and relative growth rate, *Global Change Biol.*, 5(6), 679–691.
- Tjoelker, M. G., J. Oleksyn, and P. B. Reich (2001), Modelling respiration of vegetation: Evidence for a general temperature-dependent Q₁₀, *Global Change Biol.*, 7(2), 223–230.
- Tjoelker, M. G., J. Oleksyn, P. B. Reich, and R. Zytowskiak (2008), Coupling of respiration, nitrogen, and sugars underlies convergent temperature acclimation in *Pinus banksiana* across wide-ranging sites and populations, *Global Change Biol.*, 14(4), 782–797.
- Tjoelker, M. G., P. B. Reich, and J. Oleksyn (1999b), Changes in leaf nitrogen and carbohydrates underlie temperature and CO₂ acclimation of dark respiration in five boreal tree species, *Plant Cell Environ.*, 22(7), 767–778.
- Wager, H. G. (1941), On the respiration and carbon assimilation rates of some arctic plants as related to temperature, *New Phytologist*, 40, 1–19.
- Waring, R. H., J. J. Landsberg, and M. Williams (1998), Net primary production of forests: A constant fraction of gross primary production? *Tree Physiol.*, 18(2), 129–134.
- Waring, R. H., and N. McDowell (2002), Use of a physiological process model with forestry yield tables to set limits on annual carbon balances, *Tree Physiol.*, 22(2–3), 179–188.
- von Wehrden, H., J. Hanspach, K. Ronnenberg, and K. Wesche (2010), Inter-annual rainfall variability in Central Asia: A contribution to the discussion on the importance of environmental stochasticity in drylands, *J. Arid Environ.*, 74(10), 1212–1215.
- Wilks, D. S. (2006), *Statistical Methods in the Atmospheric Sciences*, 627 pp., Academic Press, Amsterdam.
- Wright, I. J., et al. (2004), The worldwide leaf economics spectrum, *Nature*, 428(6985), 821–827.
- Wythers, K. R., P. B. Reich, M. G. Tjoelker, and P. B. Bolstad (2005), Foliar respiration acclimation to temperature and temperature variable Q₁₀ alter ecosystem carbon balance, *Global Change Biol.*, 11(3), 435–449.
- Zaragoza-Castells, J., D. Sanchez-Gomez, I. P. Hartley, S. Matesanz, F. Valladares, J. Lloyd, and O. K. Atkin (2008), Climate-dependent variations in leaf respiration in a dry-land, low productivity Mediterranean forest: The importance of acclimation in both high-light and shaded habitats, *Funct. Ecol.*, 22(1), 172–184.